Proc. of the European Safety and Reliability Conference (ESREL 2026)
Edited by José C. Matos, Paulo B. Lourenço, Michael Beer, Daniel Oliveira,
Edoardo Patelli, Hélder S. Sousa, Rui A. Silva and Monica Santamaria
 Published by Research Publishing, Singapore.
doi: 10.3850/ESREL2026061419_esrel26-p26365-cd

Probabilistic Risk Assessment of Bird-Turbine Collisions Using Flight Path Models

Soudabeh Shemehsavar

School of Mathematics, Statistics, Chemistry and Physics, Murdoch University, Perth, WA, Australia.
E-mail: soudabeh.shemehsavar@murdoch.edu.au

Graeme Hocking

School of Mathematics, Statistics, Chemistry and Physics, Murdoch University, Perth, WA, Australia.
E-mail: G.Hocking@murdoch.edu.au

Ross Maller

Research School of Finance, Actuarial Studies and Statistics, Australian National University, Canberra, ACT, Australia. E-mail: ross.maller@anu.edu.au

Patricia A. Fleming

School of Environmental and Conservation Sciences, Murdoch University, Perth, WA, Australia.
E-mail: T.Fleming@murdoch.edu.au

Wafaa Mansoor

School of Mathematics, Statistics, Chemistry and Physics, Murdoch University, Perth, WA, Australia.
E-mail: Wafaa.Mansoor2@murdoch.edu.au

A hybrid probabilistic framework was developed to assess bird collision risk using stochastic flight path models based on Brownian motion and Brownian bridge processes. Species-specific flight parameters for itinerant and nesting birds were derived from field surveys and radar data collected in a remote outback region of Australia. Simulations were conducted to estimate the probability of birds entering the rotor-swept area of turbines and the expected number of collisions, accounting for turbine characteristics and flight variability. The results indicate that higher expected collision numbers were generally observed for itinerant birds than for nesting birds under similar avoidance rates. For nesting birds, collision estimates obtained from the Brownian bridge model were comparable to those from the Brownian motion model but corresponded to longer flight durations.

Keywords: Wind turbine, collision risk, CRM, Brownian motion, Brownian bridge process

1. Introduction

Wind turbine farms play a crucial role in producing renewable, low-carbon energy and combating climate change, thereby contributing to cleaner air and a more sustainable future. However, while these installations are key for environmental protection, they can also create unintended impacts on wildlife. One important concern is the collision risks they pose for birds. Understanding and mitigating these risks is essential not only for conserving bird populations but also for ensuring that the transition to green energy is truly environmentally responsible. Balancing clean energy production with biodiversity conservation is a central challenge for policymakers and environmentalists.

Collision Risk Modeling (CRM) has developed over the past four decades as a key approach for assessing bird–turbine interactions. Early models relied on simple probabilistic assumptions and had few input parameters; e.g., Manning (1983) used only five parameters to estimate collision risk. As the field progressed, models increased in complexity to account for turbine geometry, bird morphology and behaviour, and to enable evaluation on the scale of entire wind farms.

A major advance was the Band et al. (2007) model, later updated by Band (2012), which remains widely used. This model incorporated detailed wind turbine specifications together with bird behavioral and morphological parameters and introduced stochastic components to represent uncertainty, particularly for flight height.

Advances in CRM approaches have been supported by improved field data, including radar and GPS tracking, which enables better characterisation of flight heights, movement patterns, and avoidance behaviour (e.g., Hull & Muir (2013); Holmstrom et al. (2011); Christie & Urquhart (2015)). Where sufficient species-specific data are available, CRM outputs inform turbine placement and buffer zone design, thereby reducing collision risk (Murgatroyd et al. (2021)).

If there is sufficient data on a particular species, the likelihood of being in the vicinity of the rotors can be estimated with some confidence. Murgatroyd et al. (2021) analyzed GPS data for the behaviour of Verreaux's eagle (*Aquila verreauxii*) and found that their most favoured habitat was in countryside with slopes to assist in their soaring. Murgatroyd et al. were able to make more confident predictions of the best locations for the turbines so as to avoid encroaching on the areas preferred by the eagles and to recommend safer places for turbines and buffer zones.

A recent synthesis by Cook et al. (2025) reviewed 52 CRM approaches published over the last 40 years. Only 23 models were sufficiently documented to allow replication, highlighting the importance of designing transparent and reproducible CRM frameworks.

Although CRM approaches vary in complexity, they share a common structure designed to:

(1) estimate the likelihood of birds occurring in the high-risk zone near turbines;
(2) estimate the probability of passing through the rotor-swept area; and
(3) estimate the probability of collision given rotor passage.

The present study introduces a probabilistic framework to assess bird-turbine collision risk using stochastic flight path models. To capture variability arising from environmental conditions and behavioural factors, two broad classes of birds are considered: itinerant birds, which move flexibly between multiple roosting locations, and nesting birds, which commute between a fixed nest and surrounding foraging areas. These movement types are represented by three probabilistic models describing the birds' flight paths. Two scenarios, motivated by field surveys and radar data collected in an outback region of Australia, are considered.

2. Methods

Simulations were used to estimate the probability of birds entering the rotor swept area and so predict the expected number of collisions. In each scenario a virtual 2-dimensional wind farm was constructed in a rectangle $\mathbf{R}$ of dimensions $[-2500, 2500] \times [-2000, 2000]$, with 10 turbines incorporating real-world rotor characteristics.

In $\mathbf{Scenario\,1}$, 1000 birds ("itinerant birds") were assumed to be located uniformly throughout $\mathbf{R}$. Each bird was assumed to fly according to a Brownian motion path, each flight being replicated 500 times.

$\mathbf{Scenario\,2}$ was prompted by observations on Australian raptors. A bird nests in a particular location in $\mathbf{R}$ and takes flight according to a Brownian bridge model. Each flight was replicated 500 times to account for variability, generating 1000 stochastic two-dimensional paths per bird.

In each scenario, a second probability model – straight-line paths with random directions – was included as a kind of baseline situation.

A wind turbine's blades rotate in the vertical plane while the turbine rotates around its axis in the horizontal plane due to shifting wind directions. Thus on average it sweeps out a *contact area* πr_B^2, where r_B is the blade length, in the plane.

In each of the two scenarios, for each simulated flight, a bird's entrance, or not, into the swept area of the turbines was recorded. The proportion of such entrances provides an estimate of the probability that a bird, located randomly in $\mathbf{R}$ (Scenario 1) or at a nest site in $\mathbf{R}$ (Scenario 2), enters the swept area of the turbines.

Multiplying this value by the probability that the bird was within the height range of the turbine blades, then further multiplying by the probability that the bird flying at the blades' height is hit by them, rather than avoiding them, gives an estimate of the collision probability. Details of these two calculations are in Sections 5 and 6.

This modelling approach combines variation in bird behavioural features with turbine features to provide a practical tool for supporting bird-safe turbine placement in wind energy development.

3. First Scenario: Part (a) Straight Line Flight Paths with Random Directions

In this scenario 1000 birds are located according to a uniform distribution in the rectangle $\mathbf{R}$. 10 turbines, each of radius 100m, are centered at $(0, 0), (0, \pm 300), (0, \pm 600), \ldots, (0, 1500)$. Each bird leaves its initial position and flies in a straight line at a random direction θ for a potential time T_{max} seconds. If the flight enters the turbine swept area before time T_{max} it ceases at that point and a "hit" is registered. Otherwise it ceases at time T_{max} and no hit is registered. A typical sample path simulation is shown in Fig. 1.

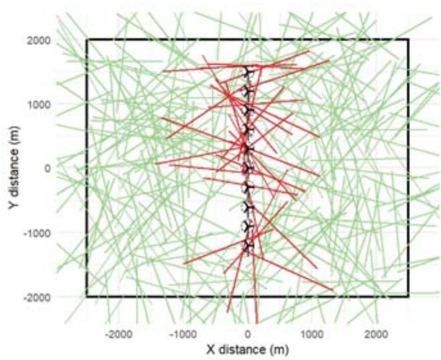

Fig. 1.: *Scenario 1(a). Straight line path, random direction. Red paths enter the turbines' swept area.*

Table 1 presents the estimated probability that a bird enters the turbine swept area, P_{swept}, based on simulations for varying flight speeds and durations. Once flights last longer than 1 hr, in this case, the probabilities remain constant, because after that time a bird has flown far enough to certainly enter the swept area, if it is headed in that direction.

Table 1.: Scenario 1(a), Straight line path, random direction, 10 turbines, estimated P_{swept}.

Speed	Flight duration (mins)				
(m/s)	1	6	60	120	240
5	0.03	0.14	0.20	0.20	0.20
10	0.05	0.19	0.20	0.20	0.20
20	0.10	0.20	0.20	0.20	0.20
30	0.14	0.20	0.20	0.20	0.20

First Scenario: Part (b) Random Walk and Brownian Motion Flight Paths

In this section the turbines and the birds' initial locations are as for Part (a) but the flight path of a bird is modelled by a random walk, approximating a Brownian motion in 2 dimensions.

Each bird leaves its initial position (X_0, Y_0) and flies at speed v m/sec for a potential time T_{max} seconds. Its flight path follows a random walk in 2 dimensions with increments (step size) $(\Delta X, \Delta Y)$ distributed as independent bivariate normal $N_2(0, \sigma^2 \Delta t)$ random vectors. Increments to the random walk take place at time steps $\Delta t, 2\Delta t, \ldots, N\Delta t$, where $N = T_{max}/\Delta t$ is the potential number of steps in the random walk. The X and Y components are assumed uncorrelated, each with variance $\sigma^2 \Delta t$.

The unknown parameter σ^2 is estimated for a given flight speed and time, using that the distance covered in a step, $D = \sqrt{\Delta X^2 + \Delta Y^2}$, has a Rayleigh distribution with expectation $\sqrt{\frac{\pi \Delta t}{2}}\, \sigma$.

This procedure simulates a flight using a random walk. By decreasing the step size the procedure approximates a Brownian motion as closely as desired. A 2-dimensional Brownian motion $(\mathbf{B}_t)_{t \geq 0}$ is a continuous time process satisfying the following stochastic differential equation:

$$\mathrm{d}\mathbf{B}_t = \boldsymbol{\mu}\mathrm{d}t + \sigma \mathrm{d}\mathbf{W}_t,\ t \geq 0, \tag{1}$$

where $\boldsymbol{\mu}$ is the direction of the motion, $\sigma^2 > 0$, and $(\mathbf{W}_t)_{t \geq 0}$ is a bivariate standard Wiener process whose components are independent univariate Wiener processes. A univariate Wiener process is a process $(W_t)_{t \geq 0}$ in continuous time such that path increments $(W_t - W_{t-s})$ are normally distributed $N(0, t-s)$ for each $t > 0$ and $0 \leq s \leq t$, and are independent. Thus W_t is normally distributed $N(0, t)$ for each $t > 0$. The process starts at $(0, 0)$ at time $t = 0$.

Random Walk Simulation Setup

The following algorithm was followed.

- Simulate the positions $(X_{0i}, Y_{0i})_{1 \leq i \leq n}$ of n birds uniformly located in $\mathbf{R}$.
- Flight time T_{max} and speed v as in Table 2.
- Time step $\Delta t = 10$ seconds.
- Distance covered each step $v\Delta t$.
- Step size $(\Delta X, \Delta Y) \sim N_2(0, \sigma^2 \Delta t)$ metres.
- Distance $D_S(i)$ covered in step i has expectation $E(D_S(i)) = \sqrt{\frac{\pi \Delta t}{2}}\sigma$.
- Equate $\sqrt{\frac{\pi \Delta t}{2}}\sigma$ to $v\Delta t$ and solve for σ.
- Number of steps is $N = T_{max}/\Delta t$.
- Position after N steps has distribution $N_2(0, N\sigma^2 \Delta t) + (X_0, Y_0)$ ($\boldsymbol{\mu} = 0$ in (1)).
- Expected distance travelled from start point $E(Rayleigh) = \sqrt{\frac{\pi T_{max}}{2}}\sigma$.
- Actual flight distance $\sum_{i=1}^{N} D_S(i)$ metres.
- Expected actual flight distance is $E(Rayleigh) = vT_{max}$ metres.

A zero-mean Brownian motion in 2 dimensions is recurrent so it will hit any given area eventually with probability 1, but the hitting time distribution has infinite mean. Random walk simulations were used to estimate the probabilities of entering the swept area prior to T_{max} for 10 turbines. Realisations of a number of paths for 10 turbines are shown in Fig.2.

The model was run for the combinations of flight speeds and durations in Table 2, with $m = 1000$ simulations. In each case, the probability P_{swept} of entering the rotor swept area was estimated as the proportion of hits among the m simulations. Flight speed and duration affect the probability of contact with the swept area in significant ways. The probability naturally increases with longer flight durations, but higher speeds also increase the likelihood of contact. The highest probability occurs at 30 m/s and 4 hours of flight. Further discussion is in Section 8.

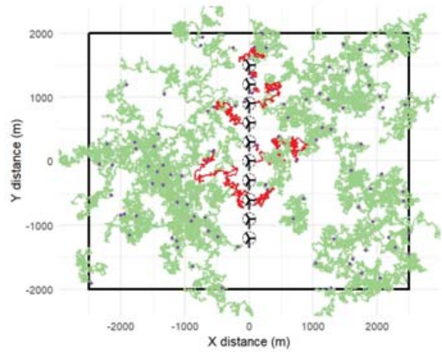

Fig. 2.: *Scenario 1(b). Brownian motion simulated paths. Only the red paths enter the turbines' swept area.*

Table 2.: Scenario 1(b). Brownian paths, 10 turbines, estimated P_{swept}.

Speed (m/s)	Flight duration (hours) 1	2	4
5	0.049	0.063	0.090
10	0.069	0.074	0.116
20	0.073	0.111	0.142
30	0.085	0.136	0.166

The values $\hat{p}$ in the tables are estimates of binomial probabilities so their standard errors are $\approx \hat{p}(1 - \hat{p})/\sqrt{1000} \approx 0.005$, so the values are accurate to about the third significant figure. (More accuracy can be obtained by increasing the number of simulations.)

4. Second Scenario: Part (a) Straight Line Paths with Random Directions

For this, flight paths were generated as in Section 3 Part (a). Table 3 gives the results of the simulations for P_{swept}. Once flights last longer than 1 hr, the probabilities remain constant.

Table 3.: Scenario 2(a), Straight line path, random direction, 10 turbines, estimated P_{swept}.

Speed (m/s)	1	Flight duration (mins) 6	60	120	240
5	0	0.08	0.153	0.153	0.153
10	0	0.153	0.153	0.153	0.153
20	0	0.153	0.153	0.153	0.153
30	0.08	0.153	0.153	0.153	0.153

Second Scenario: Part (b) Brownian Bridge Flight Path Model

Rather than Brownian motion we can model a bird's flight using a bivariate Brownian bridge (BB) process. A Brownian motion has variance at time t proportional to t, and so oscillates more and more widely as time increases, as can be seen in Fig. 2. By contrast, a BB process is constrained to both start and finish at location $(0, 0)$ (at time T_{max}, unless it enters the turbines' swept area before this). Hence it is an appropriate model for birds that nest at a particular location and return to it after a flight.

For the simulation setup a random walk with small time steps approximating a standard Brownian motion $B(t)$ was constructed as in Section 3. This was converted to an approximate standard Brownian bridge $BB(t)$ by setting

$$BB(t) = B(t) - tB(1). \qquad (2)$$

The same parameter σ^2 as for the Brownian motion was used in the simulations. See Fig. 3.

Table 4.: Scenario 2(b). Brownian bridge paths, 10 turbines, estimated probabilities P_{swept}.

Speed (km/h)	Flight duration (hours) 1	2	4
5	0	0	0
10	0	0	0.002
20	0.008	0.070	0.232
30	0.103	0.252	0.442

Table 4 gives the simulation results for P_{swept}. Next we add in the last two ingredients for estimating overall collision probabilities.

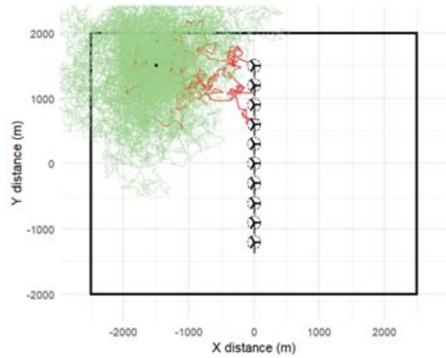

Fig. 3.: *Scenario 2(b). Brownian Bridge paths. Only the red paths enter the turbines' swept area. Birds start and finsh at this nest* $(-1500, 1500)$.

5. Height Distribution

A lognormal distribution (Fig. 4) was fitted to data on the flight heights of raptors derived from radar and survey data collected in an outback region of Australia. From this a probability $P_{\text{Height}} = 0.2712$ of a raptor flying at rotor blade height (between 100–300m) was estimated.

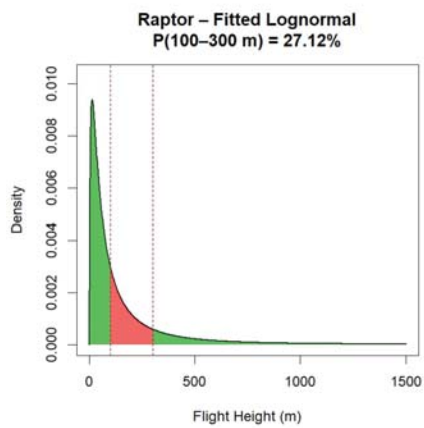

Fig. 4.: *Lognormal Height Distribution.*

6. Probability Bird Hits Turbine Blades

Suppose a bird of length L, travelling at speed v, enters the rotor disc area of a turbine whose blades have an average depth D_B (front to back). We calculate the likelihood of it being struck.

The time taken for the bird to travel from the first point of contact to the last is $t_P = (L + D_B)/v$. Suppose the turbine rotates with angular speed ω rpm (revolutions per minute). Then each cycle is completed in $60/\omega$ seconds, and the vertical area swept is $\omega_r = 2\pi\omega/60$ radians/sec. Therefore the angle through which the blade passes in time t_P is

$$A_P = t_P\omega_r = \frac{(L + D_B)2\pi\omega}{60v}.$$

There are 3 blades on the turbine, so the total angle swept in time t_P is $3A_P$. Hence the proportion of turbine blade area obstructing the bird's passage, and thus the likelihood of it being struck in flight through the rotor disk area, is

$$P_R = \frac{3A_P}{2\pi} = \frac{3(L + D_B)2\pi\omega}{60v2\pi} = \frac{(L + D_B)\omega}{20v}.$$

This computation based on a circular rotor sweep with area πr_B^2 is converted to the likelihood of a bird passing through a square window of height and width $2r_B$, thus with an area of $4r_B^2$, to give the probability of collision as

$$P_{\text{hit}} = \frac{\pi}{4}\mathcal{P}_R = \frac{\pi(L + D_B)\omega}{80v}.$$

Suppose $D_B = 3$, $L = 1$, $v = 12$, $\omega = 10$. Then

$$P_{\text{hit}} = \frac{4\pi \times 10}{80 \times 12} = 0.1309.$$

Having obtained P_{swept}, P_{height} and P_{hit} a total collision probability can be calculated as

$$P_{\text{Collision}} = P_{\text{swept}} \times P_{\text{height}} \times P_{\text{hit}}.$$

Values of $P_{\text{Collision}}$ are listed in Tables 5 – 8.

Table 5.: Total collision probabilities using P_{swept} from Table 1; random direction paths.

Speed (m/s)	Flight duration (hours) 1	2	4
5	0.022	0.022	0.022
10	0.011	0.011	0.011
20	0.005	0.005	0.005
30	0.004	0.004	0.004

Table 6.: Total collision probabilities using P_{swept} from Table 2; Brownian motion paths.

Speed (m/s)	Flight duration (hours) 1	2	4
5	0.005	0.007	0.010
10	0.004	0.004	0.006
20	0.002	0.003	0.004
30	0.001	0.002	0.003

Table 7.: Total collision probabilities using P_{swept} from Table 3; random direction paths.

Speed (m/s)	Flight duration (hours) 1	2	4
5	0.017	0.017	0.017
10	0.008	0.008	0.008
20	0.004	0.004	0.004
30	0.003	0.003	0.003

Table 8.: Total collision probability using P_{swept} from Table 4; Brownian bridge paths.

Speed (m/s)	Flight duration (hours) 1	2	4
5	0	0	0
10	0	0	0
20	0	0.002	0.006
30	0.002	0.005	0.008

7. Illustration

For illustration, we consider 100 birds under Scenarios 1 and 2, flying once per day at a mean speed of 20km/h with daily flight durations of 1 and 2 hours, assuming different avoidance rates.

Here, the *avoidance rate* refers to the proportion of birds that successfully detect and actively avoid entering the turbine swept area during flight; for example, a 75% avoidance rate implies that 25% of birds whose trajectories intersect the rotor swept area fail to avoid collision. The expected annual number of collisions under these conditions is summarized in Table 9.

Table 9.: Expected annual number of bird–turbine collisions for a mean speed of 20 m/s.

Model	Duration	Avoidance rate		
		75%	95%	99.5%
Scenario 1(a)	$\geq$ 10 min	46	9	1
Brownian	1 hour	18	4	0
Brownian	2 hours	27	5	1
Scenario 2(a)	$\geq$ 10 min	37	7	1
BB	1 hour	0	0	0
BB	2 hours	18	4	0

8. Discussion

A probabilistic framework was developed to estimate bird-turbine collision risks, motivated by field surveys and radar data collected in an outback region of Australia. In the absence of detailed species-specific data, general conclusions were drawn using stochastic flight path models that are consistent with observed movement patterns.

Two representative bird types were considered: itinerant birds exhibiting flexible roosting behavior, and nesting birds. Three flight models were employed: straight-line paths, Brownian motion, and Brownian bridges. Straight-line path models provide baseline estimates, while the stochastic models incorporate variability from environmental factors and individual behaviour.

The results in Table 9 illustrate the importance of bird type and movement assumptions in predicting collision risk. For itinerant birds, Scenario 1(a) (straight-line flight paths with random angles) predicts 46 collisions per year at a 75% avoidance rate, compared with 18 collisions predicted by the Brownian motion model for a one-hour flight. The higher risk predicted by the straight-line path model reflects the fact that straight trajectories are more likely to intersect turbine rotor areas, whereas stochastic movement introduces directional variability that may divert birds away from turbines. While the straight-line path model produces constant collision estimates for all flight durations greater than 10 minutes, the stochastic Brownian motion model shows increasing collision risk with longer flight times, as birds potentially explore a larger portion of the wind farm.

For nesting birds, Scenario 2(a) (straight-line nest-based flights) predicts 37 collisions at a 75% avoidance rate. In contrast, the Brownian bridge model predicts substantially fewer collisions for shorter flights, with no collisions expected for a one-hour flight and 18 collisions predicted for a two-hour flight. As in Scenario 1(a), the straight-line model yields constant estimates, whereas the Brownian bridge model, which constrains movement between starting and destination locations, produces lower collision probabilities for shorter durations and higher values as the potential movement range increases.

Brownian bridges have previously been used to model animal movement patterns, particularly when movement occurs between known starting and ending locations. For example, Fischer et al. (2013) used Brownian bridges to estimate home ranges for vultures equipped with satellite transmitters in South Carolina between October 2006 and November 2008. Similarly, Buchin et al. (2015) applied Brownian bridge models to analyse the movements of birds and monkeys. Brownian motion models, in contrast, have frequently been used to represent random movement patterns of animals and insects (e.g., Bearup et al., 2015). Although references specific to birds in this region are limited, theoretical hitting probability formulas for Brownian motion are available (e.g., Schencker, 2018), and it would be of interest to extend these results to turbine arrays such as the one considered here.

The simulation methodology is highly flexible. The particular scenarios considered in this study, such as ten turbines aligned within a catchment area of size R, specific bird entry locations, and assumed distributions of flight paths and heights, can be readily modified to represent other wind farm layouts or bird behaviours.

Overall, birds that travel further from their nest are more in danger of collision than those which stay relatively close by, since they are more likely to reach the vicinity of the turbines. This risk depends on the distance of the nest from the turbines, and a straight-line flight is more likely to intersect the line of turbines than a winding path generated by Brownian motion or Brownian bridge models.

These findings emphasise the importance of collecting behavioural and nesting data, especially for large wind farms, in order to inform turbine placement and mitigate risks to the most vulnerable bird species.

Acknowledgement

We are pleased to acknowledge the support of the Fortescue Metals Group, Perth, Australia and the Harry Butler Institute, Murdoch University, Perth, Australia. Thanks also to a referee for suggesting improvements.

References

Band, W.T., Madders, M. & Whitfield, D.P. (2007) Developing field and analytical methods to assess avian collision risk at wind farms. In: *Birds and Wind Farms: Risk Assessment and Mitigation*, Ch. 15, pp. 259-275, Quercus, Madrid.

Band, W.T. (2012) Using a collision risk model to assess bird collision risks for offshore windfarms. SOSS Report. British Trust for Ornithology and The Crown Estate.

Bearup, D., Benefer, C.M., Petrovskii, S.V., Blackshaw, R.P. (2015) Revisiting Brownian motion as a description of animal movement: a comparison to experimental movement data Methods Ecol. Evol, 7: 1525-1537.

Buchin, K., Sijben, S., van Loon, E., Sapir, N., Mercier, S., Arseneau, J.M. & Willems, E.P. (2015) Deriving movement properties and the effect of the environment from the Brownian bridge movement model in monkeys and birds. Movement Ecol., 3, Article 18.

Christie, D. & Urquhart, B. (2015). A refinement of the Band spreadsheet for wind turbine collision risk allowing for oblique entry. New Zealand J. Zoology, 42, 290-300.

Cook, A.S.C.P., Salkanovic, E., Masden E., Lee, H.E. & Kiilerich, A.H. (2025) A critical appraisal of 40 years of avian collision risk modelling: How have we got here and where do we go next? Environmental Impact Assessment Review, 110, 107717.

Fischer, J.W., Walter, W.D. & Avery, M.L. (2013) Brownian Bridge movement models to characterize birds' home ranges. The Condor 115, 298–305.

Heinsalu, E., Hernandez-Garcıa, E. & Lopez, C. (2010) Spatial clustering of inter-acting bugs: Lévy flights versus Gaussian jumps. Europhysics Letters, 92, 40011.

Holmstrom, L., Hamer, T., Colclazier, D.E., Verschuyl, N. & Ruché, J. (2011) Assessing avian-wind turbine collision risk: an approach angle dependent model. Wind Engineering 35, 289–300.

Hull, C. & Muir, S. (2013) Behaviour and turbine avoidance rates of eagles at two wind farms in Tasmania, Australia. Wildlife Society Bulletin, 37, 49-58.

Humphries, G., et al. (2013) The 'stochLAB' R package.

Manning (1983) The environmental impact of the use of large wind turbines. Environ. Sci., 1-11.

Masden, E. (2015) Developing an avian collision risk model to incorporate variability and uncertainty. Scottish Mar. Fresh. Science, 6, 14.

Mathai, A.M. (1999) *An Introduction to Geometrical Probability.* Gordon & Breach, Science Pub., Amsterdam.

Murgatroyd, M., Bouten, W. & Ama, A. (2021) A predictive model for improving placement of wind turbines to minimise collision risk potential for a large soaring raptor. J. Appl. Ecology, 58, 857-868.

Schenker, J. (2018) Trapping planar Brownian motion in a non circular trap. ALEA, Latin Amer. J. Probab. Math. Stat., 15, 213–231.